Quantum Hall response to time-dependent strain gradients in graphene: Supplementary Material

PROGRAMMABLE GAUGE FIELDS

We briefly review the relation between strain fields and synthetic gauge fields in the geometry of Zhu *et. al.* [1], and obtain some further useful formulas specifically for the pseudoelectric field. Consider applying a force F along the y direction in Fig. 1 in the main text. It leads to a stretch by Δy. Force balance along any cut at constant y implies $F = W(y)hY\epsilon_{yy}(y)$ where $\sigma_{yy}(y) = Y\epsilon_{yy}(y)$ is the stress along y, h is the "width" of graphene, and Y is the Young modulus. This implies a y-dependent strain controlled by the width function $W(y)$,

$$\epsilon_{yy}(y) = \frac{F}{hY}\frac{1}{W(y)}. \tag{1}$$

Thus, a narrowing width yields a strain gradient

$$\frac{\partial \epsilon_{yy}}{\partial y} = -\frac{F}{hY}\frac{\frac{\partial W(y)}{\partial y}}{W(y)^2}. \tag{2}$$

In order to obtain a constant gradient $\frac{\partial \epsilon_{yy}}{\partial y}$ one needs to choose a specific width function, given by

$$W(y) = \frac{f_r L}{f_r(L-y)+y}W(0), \tag{3}$$

where $f_r = \frac{W(L)}{W(0)}$.

One can relate the force and the stretch Δy. Using $\Delta y = \int_0^L \epsilon_{yy}(y)dy$, and Eqs. (1) and (3), we have

$$\Delta y = L\frac{F}{hY}\frac{1+f_r}{2f_r W(0)}. \tag{4}$$

Next we would like to obtain all the strain tensor components in order to calculate the pseudo vector potential from Eq. (1). We use the constitutive relations $\sigma_{xx} = \frac{Y}{1-\bar{\nu}^2}(\epsilon_{xx} + \bar{\nu}\epsilon_{yy})$, $\sigma_{yy} = \frac{Y}{1-\bar{\nu}^2}(\epsilon_{yy} + \bar{\nu}\epsilon_{xx})$, and $\sigma_{xy} = 2G\epsilon_{xy}$, as well as stress equilibrium $\sum_{i=x,y}\partial_i\sigma_{ij} = 0$. Here $\bar{\nu}$ is the Poisson ratio, and $G = \frac{E}{2(1+\bar{\nu})}$ the shear modulus. Assuming uniaxial stretch we have

$$\epsilon_{xx} + \bar{\nu}\epsilon_{yy} = 0. \tag{5}$$

Combining these relations one obtains [1] $\frac{\partial \epsilon_{xy}}{\partial y} = 0$ and $\frac{\partial \epsilon_{xy}}{\partial x} = -(1+\bar{\nu})\frac{\partial \epsilon_{yy}}{\partial y}$. For $\frac{\partial \epsilon_{yy}}{\partial y} = \text{const}$ we have

$$\epsilon_{xy}(x,y) = -(1+\bar{\nu})\frac{\partial \epsilon_{yy}(x,y)}{\partial y}x. \tag{6}$$

Thus, we determine the synthetic gauge fields in the device using Eq. (1) in the main text,

$$A_x = -c(1+\bar{\nu})\epsilon_{yy}, \quad A_y = -2c\epsilon_{xy}, \tag{7}$$

where $c = \frac{t\beta}{ev_F}$.

Consider an adiabatic time-dependent force of the form $F(t) = F_{DC} + F_{AC}\cos(\omega t)$. Using Eq. (1) and the above relations we have

$$\begin{aligned} B(x,y,t) &= 3c(1+\bar{\nu})\partial_y\epsilon_{yy} = -3c(1+\bar{\nu})\frac{F}{hY}\frac{\partial_y W(y)}{W(y)^2}, \\ E_x(x,y,t) &= c(1+\bar{\nu})\partial_t\epsilon_{yy} = c(1+\bar{\nu})\frac{\partial_t F}{hY}\frac{1}{W(y)}, \\ E_y(x,y,t) &= 2c\partial_t\epsilon_{xy} = 2c(1+\bar{\nu})\frac{\partial_t F}{hY}\frac{\partial_y W(y)}{W(y)^2}x. \end{aligned} \tag{8}$$

Relating F to the stretch $\Delta y(t) = \Delta y + \sin(\omega t)\Delta y_{AC}$ using Eq. (4), and here ignoring Δy_{AC}, gives

$$B = \left(\frac{\Delta y}{L}\right)\left(\frac{1-f_r}{1+f_r}\right)\frac{1}{L}\times 6c(1+\bar{\nu}). \tag{9}$$

The first, second, and third factors show the relation between the pseudomagnetic field and the relative stretch, the narrowing percentage, and the overall dimensions of the ribbon. The last dimensionfull factor can be estimated for graphene using $\frac{t}{ev_F} \approx 2.5\mu$m T. For a relative stretch of 20%, $f_r = 1/2$, and $L = 1\mu$m, as in Fig. 2 in the main text, as well as $\beta \approx 2.5$ and $\bar{\nu} = 0.17$, this estimate gives 3 Tesla, consistent with our COMSOL simulation.

Similarly, the pseudoelectric field along x reads

$$E_x(y,t) = \left(\frac{\Delta y_{AC}}{L}\right)\omega\left(\frac{1}{1+f_r}\frac{W(L)}{W(y)}\right)\times 4(1+\bar{\nu})c\cos(\omega t). \tag{10}$$

Note its y dependence as given by $W(y)^{-1} \propto f_r(L-y)+y$ from Eq. (3), consistent with our COMSOL simulations in Fig. 2(b),(c) in the main text.

SUPPRESSING INTERVALLEY SCATTERING USING SMOOTH EDGES

The pseudo QH effect described in this paper strongly relies on the absence of intervalley scattering. Intraedge intervalley relaxation will suppress the current by a factor $\sim e^{-L/L_{\rm iv}}$ where L is the length of the edge and $L_{\rm iv}$ is the intervalley scattering length.

We argue that this assumption can be satisfied in the modified device in Fig. 1. The idea is that any sort of edge physics on the atomic scale, which typically contains an irregular combination of zigzag and armchair edges, produces intervalley scattering. However one can push

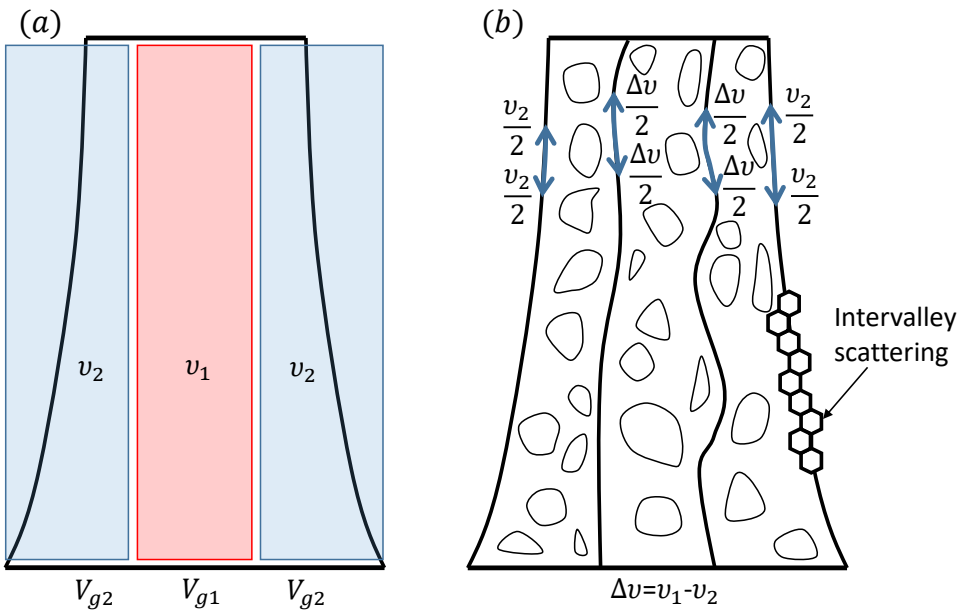

FIG. 1. Device designed to suppress intervalley scattering at the effective edges. (a) Adding parallel gates allows one to define three parallel regions in the quantum Hall regime with different filling factors. (b) Schematic electron trajectories in the presence of the disorder potential, which is assumed to be smooth on the atomic scale. The exterior edge states are sensitive to the graphene termination which is expected to cause intervalley scattering, while the internal interface modes are only sensitive to the smooth potential and hence preserve the valley index. The total number of edge modes at each edge or interface are indicated, and are equally split among the two chiralities.

the effective edges into the interior of the device, where their scattering becomes dominated by the disorder potential stabilizing the QH effect [2, 3] whose characteristic length scale is typically assumed to significantly exceed the atomic distance. As a result, the trajectories in the interior of the sample will have an approximately conserved valley quantum number.

Consider adding three gates along the device as shown in Fig. 1(a), allowing independent control of the density in the three regions. We envision these regions to stabilize separate gapped QH states, with the filling factor in the central region being $\nu_1 (= \pm 2, \pm 6, \pm 10 \dots)$, controlled by V_{g1}, and $\nu_2 \neq \nu_1$ in the exterior regions which is controlled by V_{g2}. In the bulk, the QH states consist of localized states, and the different QH states are separated by extended states, as shown in Fig. 1(b) where the typical disorder length exceeds the atomic scale. While the external edge mode trajectories between the ν_2 region and vacuum are sensitive both to bulk disorder and to atomically sharp irregularities of the physical edge of the graphene sample, the interface edge modes between the ν_1 and ν_2 regions are determined solely by the smooth disorder potential. These two types of 1D modes are spatially separated by the ν_2 gapped QH region of localized states.

The filling factors dictate the number of edge modes at each interface. For a real magnetic field the number of chiral edge modes is given by the filling factor ν, or by the difference of filling factors at an interface between two different QH states. But for a pseudomagnetic field these modes are equally split at each edge into the two chiralities, i.e., there are $\nu/2$ modes moving in each direction. As denoted in Fig. 1(b) the number of edge modes of each chirality is $\nu_2/2$ at the exterior edge and $|\nu_1 - \nu_2|/2$ at the interior interface between ν_1 and ν_2 filling factors. Let us assume $\nu_1 \geq \nu_2 > 0$ for simplicity.

Without intervalley scattering anywhere, the total two-terminal conductance as determined by the number of modes is dictated by the largest filling factor

$$\frac{I}{V_{\rm ext}}|_{\rm no\ iv\ scattering} = \frac{e^2}{h}\nu_1. \tag{11}$$

In the presence of strong intervalley scattering we assume that the external edge modes of the ν_2 region are gapped out and do not contribute. Then

$$\frac{I}{V_{\rm ext}}|_{\rm strong\ iv\ scattering} = \frac{e^2}{h}(\nu_1 - \nu_2). \tag{12}$$

As a function of the gate voltage V_{g1} controlling ν_1 the conductance will exhibit nearly quantized plateaus. The AC pseudo QH effect will follow a similar behavior.

This analysis also implies that one can use such a device to probe the importance of intervalley scattering at the outer edge and test the length scale $L_{\rm iv}$.

AC PSEUDO HALL CURRENT IN THE DIFFUSIVE REGIME

As the density is tuned through the extended PLL states, bulk transport takes place. This means that the pseudoelectric field leads to a finite valley current perpendicular to the edges of the sample. Since the electric field is opposite for the two valleys, this leads to a valley polarization near the edges, which eventually in the DC limit leads to a diffusive current effectively screening the external pseudo-E field and suppressing I. For finite frequency, this opposing diffusive current does not fully develop. We next present an approximate semiclassical analysis of the current at finite frequency.

We comment on the validity regime of our semiclassical approach which does not capture quantum effects associated with the large pseudo-magnetic field, as opposed to a full quantum transport approach e.g. using the Kubo formula. In the QH plateaus the conductance is quantized, and one does not expect to gain significant extra information from a fully quantum Kubo formula approach. In the QH transitions on which we are now interested, the localization length ξ diverges. While at zero temperature the critical behavior is cut-off by the system size (L, W), at finite temperatures there is an additional dephasing length L_ϕ smearing the QH transition (see for example [3, 4]). Our semi-classical approach below is valid for finite temperature such that $L, W \gg L_\phi$, which we assume. On the other hand, a full Kubo formula approach would be necessary to capture the physics at the QH transition for length scales smaller than L_ϕ.

We consider a transport equation for the current densities of the two valleys $\vec{j}_\pm$, which includes a dissipative conductance σ, a diffusion current, and a Hall effect, as well as the continuity equation,

$$\vec{j}_\pm = \pm\sigma\vec{E}(t) - D\vec{\nabla}n_\pm \mp (\omega_c\tau)\vec{j}_\pm \times \hat{z}, \tag{13}$$

$$0 = \vec{\nabla}\cdot\vec{j}_\pm + \frac{dn_\pm}{dt}. \tag{14}$$

Here D is the diffusion constant. The currents $\vec{j}_\pm$ and the densities $n_\pm$ are related by the continuity Eq. (14), and also satisfy boundary conditions $j_x(x=0,y) = j_x(x=W,y) = 0$. Again here we ignore intervalley scattering and hence obtain uncoupled equations for the two valleys.

We solve these equations under simplifying assumptions of (i) no $y-$dependence of neither the width $W(y) \to W$ nor the fields $E(y) \to E$, and (ii) the AC electric field points along the x direction only. Then the y component of Eq. (13) gives $j_y = \omega_c\tau j_x$, with $j_{x,y} \equiv (j_+)_{x,y}$, and the x component of Eq. (13) yields the differential equation

$$[1+(\omega_c\tau)^2]j_x = \sigma E + \frac{D}{i\omega}\partial_x^2 j_x, \tag{15}$$

with boundary condition $j_x(0) = j_x(W) = 0$. The electric field is the real part of $Ee^{i\omega t}$ and the current contains both in and out of phase components. From the diffusion time across the width of the sample

$$\tau_T \equiv \frac{W^2}{D}, \tag{16}$$

we form a dimensionless parameter $\omega\tau_T$ (which takes very low values in our system as estimated below). One recasts the differential equation in terms of dimensionless coefficients, a dimensionless variable $\tilde{x} = x/W$, and a source term,

$$j_y = \frac{\omega_c\tau}{1+(\omega_c\tau)^2}\sigma E + \frac{1}{i(\omega\tau_T)(1+(\omega_c\tau)^2)}\nabla_{\tilde{x}}^2 j_y, \tag{17}$$

with boundary conditions $j_y(\tilde{x}=0) = j_y(\tilde{x}=1) = 0$. It is solved by

$$j_y(x,t) = \frac{\sigma E(\omega_c\tau)}{1+(\omega_c\tau)^2} \times \tilde{j}(x/W)$$

$$\tilde{j}(\tilde{x}) = 1 + \left[\frac{e^{-A}-1}{e^A - e^{-A}}e^{A\tilde{x}} + (A \to -A)\right], \tag{18}$$

where $A^2 = i(\omega\tau_T)[1+(\omega_c\tau)^2]$. Having solved for j_+ (valley K), we can obtain $\vec{j}_-$ by replacing $B \to -B$ and $E \to -E$. Flow lines and the current profile as function of $\tilde{x}$ are plotted in Fig. 2.

At high frequency screening does not have time to develop. With $A \to \infty$ we have $j_y(x,t) = \frac{\sigma E(\omega_c\tau)}{1+(\omega_c\tau)^2}$, except

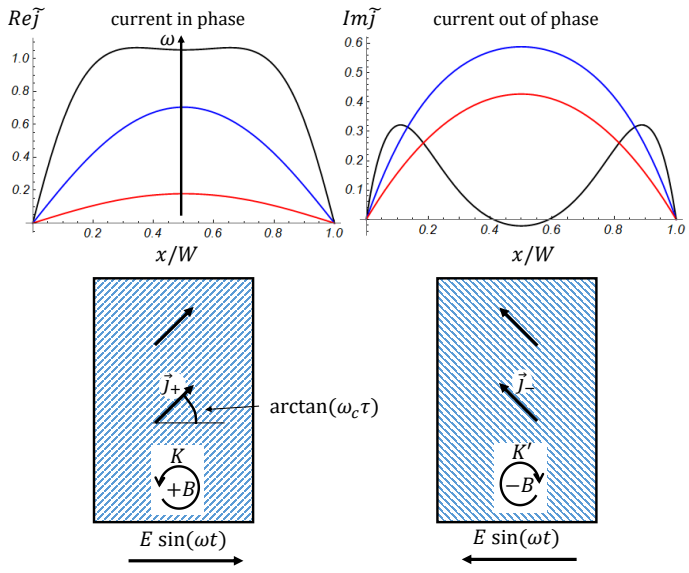

FIG. 2. Plot of the current distribution Eq. (18) in the diffusive regime as function of frequency ω. The parameter $A \propto \omega$ takes the values $10, 3.3, 2$. In the high-frequency regime the current is in phase with the electric field, except near the boundaries, since screening is not effective. At low frequencies we obtain the parabolic current distribution in Eq. (19) which is primarily out of phase.

right on the edge. This current is in phase with the electric field.

At low frequency we expect a strong suppression of the current due to screening. Expanding the solution for small A, corresponding to low frequency, we obtain

$$j_y \xrightarrow[\omega\tau_T \ll 1]{} \frac{i}{2}\sigma E \cdot (\omega_c\tau)\cdot(\omega\tau_T)\cdot\frac{x}{W}\left(\frac{x}{W}-1\right), \quad (19)$$

which is out of phase with respect to the electric field. We see the suppression factor $(\omega\tau_T)$ due to the scrreening effect, which becomes efficient when $\omega\tau_T \ll 1$. Integrating over the width of the sample yields

$$I = \int_0^W dx j_y(x) = \frac{i}{12}\sigma E W \cdot (\omega_c\tau)\cdot(\omega\tau_T). \quad (20)$$

We now estimate the diffusion time $\tau_T = W^2/D$ for a width $W \approx 0.5\mu$m. For the diffusion coefficient D we use Einstein's relation $\sigma = De^2 dn/dE_F$ with $\sigma \approx \frac{e^2}{h}$ a typical value for the longitudinal conductivity at QH transitions [5, 6]. Here we estimate dn/dE_F very crudely by assuming a density of states of a clean LL, $\frac{B}{\Phi_0}\delta(E-E_{LL})$, spread due to disorder over an energy given by the LL spacing $\hbar\omega_c = v_F\sqrt{\hbar eB}$. This estimate is equivalent as an order of magnitude to the Dirac density of states $dn/dE_F = \frac{2}{\pi}\frac{k_F}{\hbar v_F}$ with k_F determined from the electronic density of a full LL, $k_F^2 \sim \frac{B}{\Phi_0}$. For $B = 3$T this gives $k_F \sim 10^2\mu\text{m}^{-1}$ and we obtain $D \sim 0.01\text{m}^2 s^{-1}$ giving a time of $\tau_T \approx 10^{-10}$ s. For a typical piezoelectric-mechanical frequency $\omega \approx 10^7$Hz we have $\omega\tau_T \sim 10^{-3}$.

[1] S. Zhu, J. A. Stroscio, and T. Li, Phys. Rev. Lett. **115**, 245501 (2015).

[2] R. Prange and S. Girvin, Springer New York (1990).

[3] Y. Imry, *Introduction to mesoscopic physics* (Oxford University Press, 2002).

[4] H. Wei, D. Tsui, M. Paalanen, and A. Pruisken, Phys. Rev. Lett. **61**, 1294 (1988).

[5] K. S. Novoselov, A. K. Geim, S. Morozov, D. Jiang, M. Katsnelson, I. Grigorieva, S. Dubonos, and A. A. Firsov, Nature **438**, 197 (2005).

[6] S. D. Sarma, S. Adam, E. Hwang, and E. Rossi, Rev. Mod. Phys. **83**, 407 (2011).